Citation: Molecular Therapy — Methods & Clinical Development (2015) **2,** 15001; doi:10.1038/mtm.2015.1

www.nature.com/mtm

ARTICLE

Efficacy of irreversible electroporation in human pancreatic adenocarcinoma: advanced murine model

Prejesh Philips[1], Yan Li[1], Suping Li[1], Charles RS Hill[1] and Robert CG Martin[1] [Q1]

Irreversible electroporation (IRE) is a promising cell membrane ablative modality for pancreatic cancer. There have been recent concerns regarding local recurrence and the potential use of IRE as a debulking (partial ablation) modality. We hypothesize that incomplete ablation leads to early recurrence and a more aggressive biology. We created the first ever heterotopic murine model by inoculating BALB/c nude mice in the hindlimb with a subcutaneous injection of Panc-1 cells, an immortalized human pancreatic adenocarcinoma cell line. Tumors were allowed to grow from 0.75 to 1.5 cm and then treated with the goal of complete ablation or partial ablation using standard IRE settings. Animals were recovered and survived for 2 days ($n = 6$), 7 ($n = 6$), 14 ($n = 6$), 21 ($n = 6$), 30 ($n = 8$), and 60 ($n = 8$) days. All 40 animals/tumors underwent successful IRE under general anesthesia with muscle paralysis. The mean tumor volume of the animals undergoing ablation was 1,447.6 $mm^3 \pm 884$). Histologically, in the 14-, 21-, 30-, and 60-day survival groups the entire tumor was nonviable, with a persistent tumor nodule completely replaced fibrosis. In the group treated with partial ablation, incomplete electroporation/recurrences ($N = 10$ animals) were seen, of which 66% had confluent tumors and this was a significant predictor of recurrence ($P < 0.001$). Recurrent tumors were also significantly larger (mean 4,578 $mm^3 \pm$ SD 877 versus completed electroporated tumors 925.8 ± 277, $P < 0.001$). Recurrent tumors had a steeper growth curve (slope = 0.73) compared with primary tumors (0.60, $P = 0.02$). Recurrent tumors also had a significantly higher percentage of EpCAM expression, suggestive of stem cell activation. Tumors that recur after incomplete electroporation demonstrate a biologically aggressive tumor that could be more resistant to standard of care chemotherapy. Clinical correlation of this data is limited, but should be considered when IRE of pancreatic cancer is being considered. [Q2]

Molecular Therapy — Methods & Clinical Development (2015) **2**, 15001; doi:10.1038/mtm.2015.1; published online 00 Month 2015

INTRODUCTION

Electroporation is energy delivery by which cell membrane integrity is compromised by inducing nanopores through transmembrane electrical distortion. This was initially used to increase the permeability of the cells to load therapeutic compounds and gene transfer in a reversible fashion. Subsequently, it has been used as an independent cellular ablation modality to achieve permanent cell destruction and induce cellular apoptosis in animal[1] and human patients.[2–5] These studies confirmed that cell death occurred without breaching structural integrity and leaving vascular structures unharmed.[6] However, there continues to be a belief with the advent of this technology in the efficacy of "debulking" pancreatic cancer.[7,8] We have significant concern with this belief and additional concerns that partial pancreatic therapy could lead to a change in biology.

We and other authors have recently demonstrated the safe use of IRE around vascular and ductile structures on large animal models.[1,9,10] Subsequent to those studies we have recently published organ specific safety and efficacy data with the use of IRE in liver and pancreas.[2,4,5] As with any novel technology in clinical practice, initial experience can be used to tailor subsequent indications, applications and strategies to limit the morbidity of the procedure.

It is in this context that we evaluated the *in vivo* model for IRE ablation of soft tissue tumors. There are no validated irreversible electroporation pancreatic or liver tumor models currently. In this study, we optimized an animal model for ablation to evaluate the efficacy of electroporation, the optimal dosing and pulses of energy delivery, the effect on surrounding tissues, recurrence, and biomarker expression changes in recurrent/incompletely electroporated tumors.

RESULTS

Tumor inoculation and growth curve analysis

A total of 40 animals were inoculated with the tumor, in three separate sessions of 15–17 animals injected at each session, of which 4 did not develop subcutaneous tumors and were later reinjected and developed tumors. Including reinjection, all 40 animals developed subcutaneous tumors. The animals' median BCS score remained 3 throughout the parameters of the study. The tumor volume was plotted using the maximal length and width, as measured with a Verniers calipers weekly, and a growth curve over time was plotted. [Q3]

At the time of treatment, 12 additional animals were set aside as timed controls. They would serve as untreated but similar time and

[1]Division of Surgical Oncology, Department of Surgery, University of Louisville, Louisville, Kentucky, USA. Correspondence: RCG Martin (Robert.Martin@louisville.edu) [Q4]
Received 5 September 2014; accepted 22 December 2014

size controls to the treated (ablated) tumors. There were 40 animals in the test arm. On average tumors were apparent after about 2–4 weeks and achieved tumor sizes of about 1.5 cm at about 6 weeks. In some cases, we saw doublets of tumors within close proximity to each other and we attribute this to probable inoculation spread over a larger area. The postinoculation tumor growth curve followed a linear equation in all three groups (in relation to their injection session) (Figure 1a), which can be best described by the following growth curve $y = 6.3062(x) - 53.352$ with an $R^2 = 0.65$.

There were a total of three outliers from the initial part of the study on this volume curve and two of them had multiple tumors (Figure 1b). This happened early in the study and we attribute it to faulty injection technique. Overall the growth curve of the Heterotopic model was predictable albeit slow. The *in vitro* doubling time for Panc-1 cells is reported to be 32 hours. Based on the growth curve, the doubling time *in vivo* is close to 4 days. Median time to detection of tumor was 4 (IQR: –5) weeks and if tumors hadn't developed by week 8, we declared it a failed injection.

In the control group, there were 12 animals who were allowed to grow tumors till they reached preset times after 6 weeks of tumor injection, at which time they were sacrificed and tumors analyzed. Their distribution is as follows: 2 days after optimal tumor size (n = 5), 7 days after optimal tumor size (n = 1), 14 days (n = 0), 21 days (n = 1), 30 days (n = 1), and 60 days (n = 1) days. Three animals did not survive to their set points and had worsening general clinical condition and were euthanized. These animals were not used for comparison since we could not objectively place them in preset time groups.

IRE treatment outcomes

In the test group, 1 animal (out of 40) was sequestered for poor clinical condition unrelated to the injection, with a suspected infection and was quarantined. The remaining 39 animals, which were in good clinical condition, were selected for anesthesia and IRE. Animals that were selected for tumor ablation had tumors ~1 cm or greater. There was no upper size limit; however, larger tumors needed greater ablation times. Thirty-nine animals underwent successful induction of general anesthesia using isoflurane and muscle relaxation. As explained in the Materials and Methods section, the first 12 mice underwent a muscle relaxation using Pancuronium at a dose of 0.2 milligrams per kilogram, and the remaining mice received succinylcholine. All animals underwent orotracheal intubation, complete muscle relaxation and mechanical ventilation. Three animals died during the procedure. One had a cardiac arrest before we began the IRE and other two had significant airway edema after a traumatic intubation attempt.

The overall median size of the tumors at the time of ablation in X (axial length) was 1 cm (IQR: 0.9, 1.4, range: 0.6–2) and the mean 1.09 cm (SD: 0.41). The overall median size of the tumors at the time of ablation in Y (transverse breadth) was 1 cm (IQR: 0.8, 1.3, range: 0.4–1.7) and the mean 0.99 cm (SD: 0.38). The overall median dimension of the tumors at the time of ablation in Z (depth) was 0.8 cm (IQR: 0.6, 1.0, range: 0.4–1.3) and the mean 0.81 cm (SD: 0.32). As noted earlier in Methods, volumetric analysis was performed using this formula: $V = \pi/6 \times f \times (\text{length} \cdot \text{width})^{3/2}$. The "f" constant for male BALB/c mice as established in a previous study was 1.69. We chose to use the two-dimensional method of evaluation since the depth measurement for growth curve was inconsistent based on how closely the tumor adhered to underlying structures. Also it helps us assess volumes in the hemiellipsoid tumors based on slide micrographs as well or cross-sectional imaging. The median for the tumors that were ablated was 884.9 mm^2 (IQR: 540.6, 1,724.2; range: 104–4,347) and the mean was 1,386.2 mm^2.

In regards to ablation parameters, the median number of ablation treatments was 2 (range: 1–4, IQR: 2–3). Based on the tumor dimensions, the probe placement was binary and along the long axis of the largest dimension. The median distance between the two probes was 5 mm (IQR: 4, 9). All pulse settings were set at 90 pulses per minute without EKG synchronization and pulse length was 100 milliseconds. Median number of ablations per probe position was 2 (IQR: 2, 3). Based on the tumor size and shape, some tumors needed additional positioning of probes (*i.e.*, more than 1 probe pair position). Median total number of ablations, including all probe positions, was 4 (IQR: 3, 5) with a mean of 3.9. Voltage used for these ablations ranged from 600 to 1,000 V/cm, but for the majority we used 800 V/cm. In 5 of 21 animals, the ablation sequence had to be terminated and restarted due to unexpected surge in resistance. Two primary problems were identified for this. One was an inadvertent nonparallel placement of probes, which led to increased voltage at the narrow end. The other was when the tip or base of the electrode was exposed. These ablations were repeated after repositioning the probes successfully.

Post-IRE ablation outcomes

After ablation, animals were recovered and survived for predetermined times. The distribution is as follows: 2 days (n = 6), 7 days (n = 6), 14 days (n = 6), 21 days (n = 6), 30 days (n = 8), and 60 days (n = 8) days. The dimensions of the ablated tumors were analyzed and for the whole cohort the there was a positive growth rate in the postablation series of 0.025 mm^3/day or 0.175 mm^3/week. On analyzing only the successful ablations (as defined as those who completed ablations and not the incomplete ablations), the growth rate was net negative at –0.563 mm^3/week.

Hematoxylin and eosin stained (H&E) histopathological analysis of these tumors demonstrated that in control tumors that had not undergone any ablation, clearly circumscribed tumors were noted without areas of necrosis or nonviability. In contrast, ablated tumors showed progressive nonviability. Early sacrificed tumors at postprocedure day 2 (Figure 2), showed areas of nonviability (with TUNEL and H&E staining) around the ablation needle track. There was no obvious sign of thermal injury to the surrounding tumor. At postprocedure day 7, the areas of nonviability extended to the margins of the tumor and the tumor was replaced with scar and mononuclear cell infiltrate. Later (>7 days), the entire tumor was nonviable and replaced with scar tissue with fibroblastic infiltration.

Incomplete ablation/recurrent tumors and biomarker expression

Increasing postablation tumor dimensions and/or histologic presence of viable tumor cells identified recurrences/incomplete ablations. There were 10 (out of 40, 20%) tumors, which demonstrated recurrence/incomplete ablation. The growth rates of these 10 tumors prior to planned incomplete ablation were similar to the 32 complete ablation animals (Figure 1a). The distribution is as follows: 1/6 (16%) of day 7 sacrificed animals, 1/6 (16%) of day 14 sacrificed animals, 3/8 (38%) of day 30, and 3/8 (38%) of day 60 sacrificed animals. We analyzed the preablation volumes of the ablated tumors (Table 1). There was no difference in the median weight of the mice at the time of ablation between the two groups and had similar BCS scores. The recurrent tumors were significantly larger than (mean volume 4,578 mm^3 ± SD 877 versus successfully ablated tumors: 925.8 mm^3 ± 277, $P < 0.001$). They also had a higher incidence of confluent

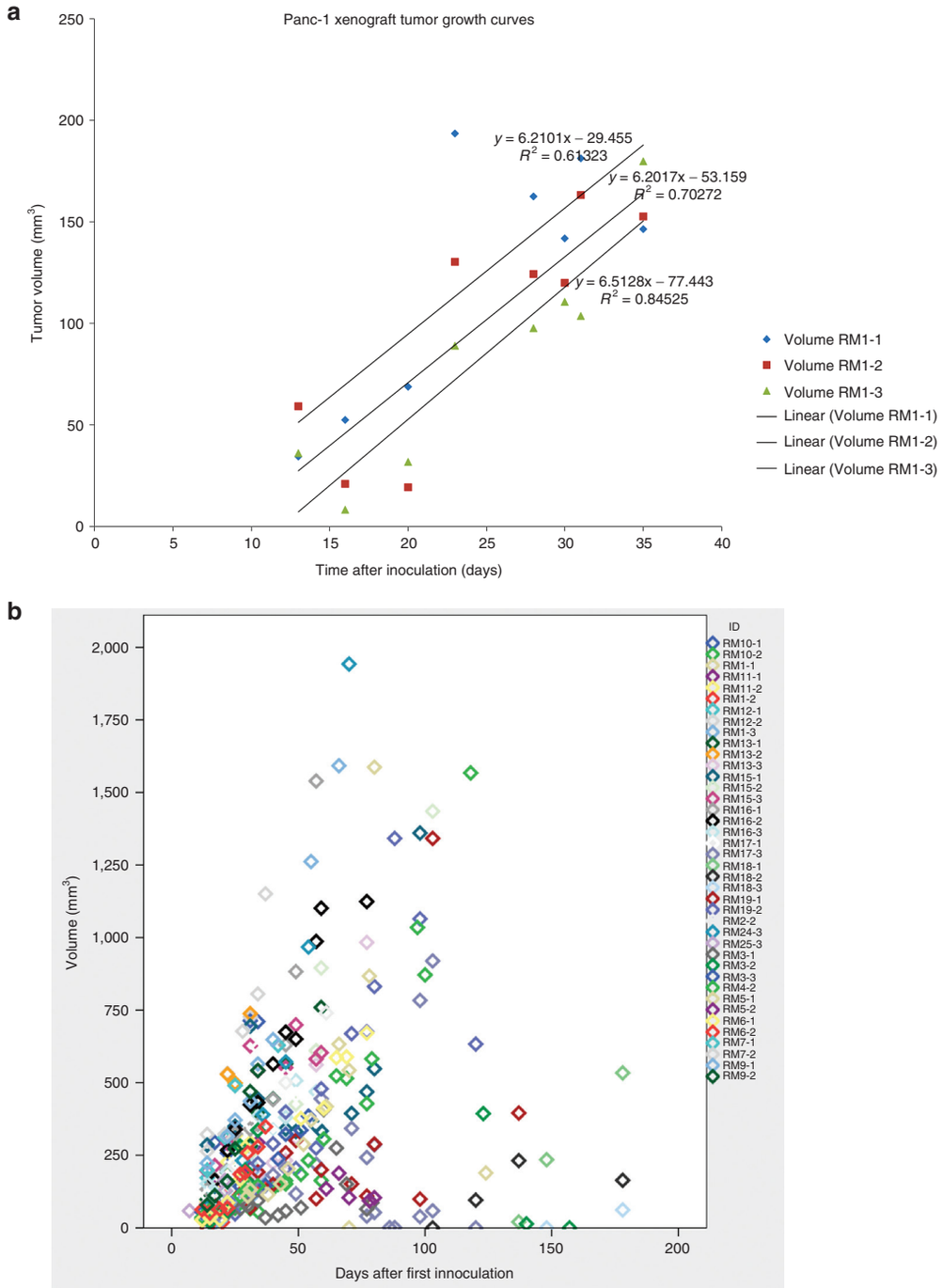

[Q5] **Figure 1** (**a**) Growth curves for all three injection sessions: RM1-1, -2, and -3 with corresponding coefficient values. (**b**) Individual tumor growth for each animal presented as tumor volume correlated to days after inoculation. [Q6]

tumors (66% versus 0, $P < 0.001$). The ablation parameters were similar with respect to voltage/cm, pulses and pulse length. However, the mean number of ablations used for the recurrent tumors were 5.33 compared to 3.7 for completely ablated tumors ($P = 0.01$). The reason more ablations had to be performed was based on the size of the tumor and the maximum spacing of the needles (5 mm), so that ~80% of the tumor was ablated to better reproduce the clinical scenario of incomplete electroporation in humans.

The recurrent/incompletely ablated tumors showed significant growth over the postprocedure observation period. They grew at a rate of median 1.8 mm^3 (range: 1.5–7.3 mm^3/day; mean 3.5) versus median of 0 (range: −7 to 0.17; mean −0.56 mm^3/day) for completely ablated tumors. This growth was significant at a P value of 0.004. We also decided to compare the rate of growth of the primary tumors to the recurrences. Recurrent tumors grew faster (slope = 0.73) than primary tumors (0.60, $P = 0.02$). An inflection point was sought and we found that only tumors >2,700 mm^3 or >15 mm in the largest dimension recurred ($P < 0.001$).

An H&E staining evaluation and immunohistochemistry (IHC) staining of these recurrent tumors was also performed. We did

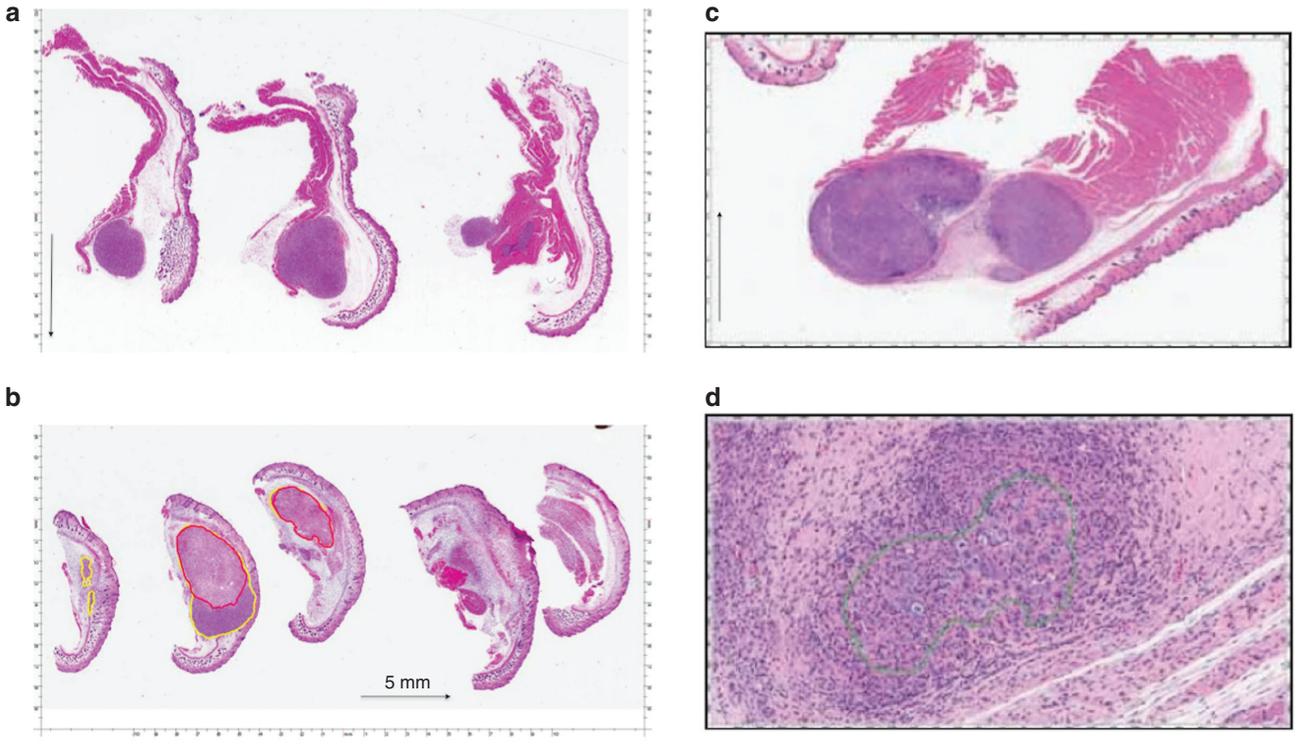

Figure 2 (**a**) Untreated control: micrograph showing viable Panc-1 human tumor xenograft from untreated control (black arrow denotes 5 mm in size). (**b**) 7 day posttreatment survival. Micrograph showing Panc-1 human tumor xenograft 7 days after IRE treatment. Using Aperio ScanScope xenograft is outlined with yellow. Nonviable tumor is outlined with red (black arrow denotes 5 mm in size). (**c**) 21 day posttreatment survival: no viable tumor present, tumor cells are surrounded by fibrosis, and mononuclear cells. There is viable muscle adjacent to tumor nodule (black arrow denotes 5 mm in size). (**d**) 21 day posttreatment survival. Shows tumor cells surrounded by chronic inflammation.

Table 1 Comparison of recurrent tumors versus completely ablated tumors

	Recurrent tumors (n = 10)	*Completely ablated tumors (n = 29)*	*Univariate analysis (P value)*
Mean dimensions X axis (in mm)	13	10	<0.001
Mean dimensions Y axis (in mm)	16	9	<0.001
Mean dimensions Y axis (in mm)	16	7	<0.001
Confluent tumors (*n*, %)	6/10, 60%	0	<0.001
Volume (mm^3)	4,578	925	<0.001
Number of total ablations	5.33	3.7	0.01
Median pulses per ablation	90	90	NA
Median voltage per ablation	800/cm	800/cm	NA
Median weight of animal at sacrifice (gm)	24.8	25.3	0.8
Mean BCS score	3	3	NA
Mean (SD) growth rate in mm^3/day	3.5 (3.3)	−0.56 (1.8)	0.004

IHC staining with EPCAM, CD24, CD44 E cadherin and Beta catenin activity. We noted that incomplete ablation/recurrence expressed significantly higher percentage of EpCAM +ve cells (by IHC staining) as compared to unablated similar tumors, suggestive of stem cell activation (Figure 3). The CD 24 and CD 44 staining was similar between the recurrent and primary tumors. Apoptotic turnover was evaluated using TUNEL staining and recurrent tumors, showing increased apoptotic turnover compared to primary tumors (Figure 3). The completely ablated tumors showed no increase in apoptotic turnover by TUNEL staining.

DISCUSSION

This study created a murine model for heterotopic implantation and development of Panc-1 cell pancreatic adenocarcinoma. As can be seen from the results we were able to successfully inject the Panc-1 cells subcutaneously into male C57BL/6, Nude BALB/c using

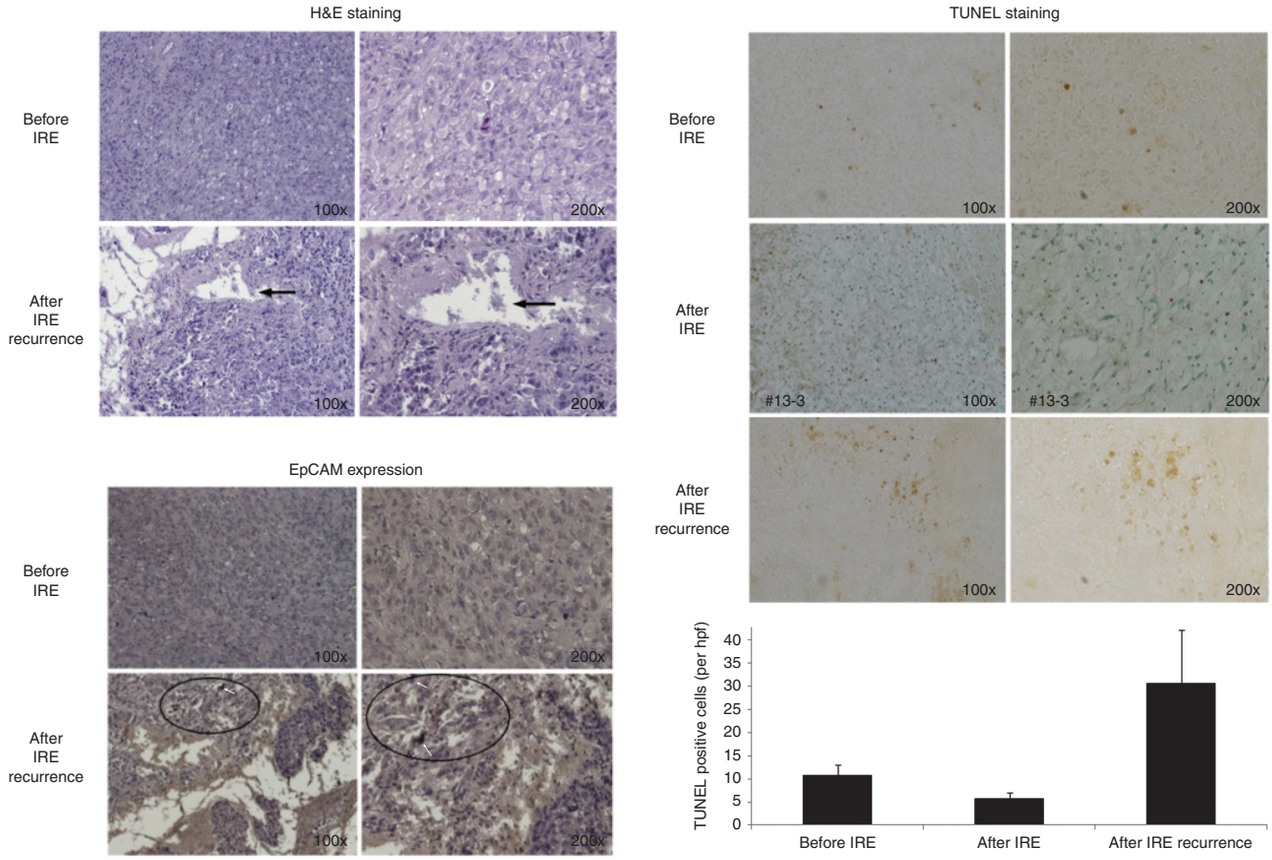

Figure 3 Histological examination of incomplete recurrences. (i) Hematoxylin and eosin staining: Areas of infiltration and necrosis (arrows) amid viable tumor cells in the recurrences (lower plate) on 100 and 200× original magnification. (ii) Immunohistochemical staining of recurrences with EpCAM antibody: Higher EpCAM expression in recurrent tumors (lower plate) compared to original Panc-1 tumors (White arrows lower panels and the example of increased EpCAM expression as defined by the deep dark brown/black cells). (iii) Higher apoptotic turnover (TUNEL staining: dark brown arrows) in IRE recurrences (middle plate) compared to original Panc-1 tumors (top plate) and completely ablated tumors (bottom plate) There is a higher EpCAM expressed cancer cells in the recurred tumors compared to the tumor of original Panc-1 cells inoculation by immunohistochemical staining (EpCAM see circles). All these features indicate that the recurrent tumor may be more aggressive than the tumor of original Panc-1 cells inoculation.

a hindlimb site. The injection protocol was safe and efficacious. Avoiding motion while injecting and not massaging the injection site helps prevent development of multiple/satellite tumors. In reviewing literature, this is one of the first murine pancreatic cancer heterotopic models using Panc-1 cells with presented growth curve rates and outcomes. We specifically chose a heterotopic hindlimb model in order to better establish growth curves of these tumors, as well as to be able to perform ablation without performing a laparotomy. This model is described in detail in our previous publication.[11]

The development of subcutaneous tumors in this model took ~4 weeks. The tumor growth after injection follows a linear path as can be seen from the growth curve calculation: $y = 6.3062(x) - 53.352$. This predictability and nonexponential nature helped us compare postablative tumor growth patterns and compare them to untreated tumors. The use of controls at specific set points helped us compare the H&E features of the untreated tumors and the treated tumors of similar age.

The number of probe pair placements was based on the size and shape of the tumor. We used a 2-probe array throughout the study in order to maintain consistency. However, as noted with tumors larger than 1.5 cm in any dimension, a multiprobe array could be used to deliver a more consistent ablation without having to reposition the probes. This could be the reason for the increased number of recurrences in the larger tumors. The needle placement had to be precisely parallel and the whole active end of the electrode had to be covered by tissue. In 5 of 21 animals, there was a spike in resistance when these conditions were not met. Three mice died during the procedure and were either intubation related ($n = 2$) or unknown cause before IRE ($n = 1$). There was no attributable mortality to IRE itself. Skin blanching over the tumor was seen in all ablations, without any permanent long-term damage to the epidermal structures. All animals had some postprocedure ipsilateral hip stiffness, which recovered by 7 days. Overall, this model if safe and reproducible. The size of tumors ablated ranged from 0.6 to 2 cm in maximum dimension. The use of controls at similar postinjection times was used to contrast the postablation tumors to primary tumors at similar time points.

A total of 10 mice, all with in the partial electroporated group, demonstrated recurrence/incomplete ablation. These tumors were significantly larger and required higher number of ablations. They also had more confluent tumors, which could be from injection artifact and could be the reason why they were larger. Tumors less than 1.5 cm or <2,700 mm^3 did not demonstrate any incidence of recurrence. The reason could be that these larger tumors required a multiprobe array for proper ablation. The rate of growth of the recurrent tumors was significantly faster than the primary tumors, which is demonstrative of a more aggressive biology. This is of particular concern based on the fact that an incomplete electroporation

can lead to a change in the biology of the tumor and thus turn a local tumor with slow growth into a more aggressive tumor with significantly greater metastatic potential (Figure 3). The recurrent tumors or incompletely ablated tumors showed more infiltrations and necrosis than primary tumors as can be expected on H&E staining. However, on TUNEL staining, there was evidence of increased apoptotic turnover as well as increased expression of EpCAM in the recurrent tumors. This is a strong indicator of the more aggressive biology of the recurrence via a cancer stem cell model, as compared to the primary tumors.

This study was not primarily designed to assess biology of recurrent tumors, although this is an area of interest for us. The lacunae associated with comparing small numbers (in the recurrent group) and not having similar sized nonablated control was therefore unavoidable. However, having the recurrences helped us identify certain size criteria for IRE using miniature animal probes and a 2-probe array.

In conclusion, this is a novel model for induction of a heterotopic Panc-1 pancreatic cancer model and subsequent soft tissue ablation using low-energy DC current. The model shows that IRE is safe and efficacious in animal model when appropriate size criteria are met. Incomplete ablation/recurrences induce a more aggressive disease biology as exhibited by faster growth rates and increased cancer stem cell markers (EpCAM) and greater apoptotic turnover. Drawing parallels to the clinical scenario, appropriate size tumors (defined as ≤3 cm)[12] should be selected for IRE and an incomplete ablation could lead to hastening the disease process and bringing about a more aggressive tumor biology.

MATERIALS AND METHODS

The study approval was obtained from the University of Louisville Institutional Animal Care and Use Committee (IACUC), and the care of all study animals were in accordance with IACUC guidelines and was conducted according to ARRIVE guidelines.

Cell line and animal selection

In order to create a locally advanced animal tumor model, we selected a recently validated Panc-1 cancer tumor cell line. Established from a pancreatic carcinoma of ductal origin from a 56-year-old Caucasian male, these cells possess the type B phenotype for Glucose-6-phosphate dehydrogenase (G6PD).[13] The Y chromosome could not be detected in this cell line by short tandem repeat (STR)-PCR analysis when tested at European collection of cell cultures (ECACC). It is a known phenomenon that due to the increased genetic instability of cancer cell lines the Y chromosome can be rearranged or lost resulting in lack of detection. The cell line is identical to the source provided by the depositor based on the STR-PCR analysis and overexpress heregulin/human epidermal growth-factor receptor 2 (HER2/neu) oncogene (which is present in 60–70% of human pancreatic carcinomas). These cells had a slow doubling time and lag time to initial tumor development was close to 4–6 weeks.[14] With the goal to assess effective tumor ablation out to 2 months, a nonmetastatic controlled tumor model was necessary to ensure local tumor ablation effectiveness and to avoid the confounding variable of metastatic disease leading to an increase in adverse events or death.

Immunologically nude mice are the least sentient species capable of growing a 1–1.5 cm tumor. To that end male C57BL/6, Nude BALB/C were selected for the experiment. A previously described Xenograft Pancreatic Tumor model, using a human pancreatic cell line, was selected.[15] This technique has been well established and confirmed as a clinically relevant and reproducible animal model for clinical evaluation of both local and systemic therapies. Animals were 8 weeks old at procurement. They were evaluated before and after innoculation using Body Condition Scoring (BCS) criteria.

Inoculation and follow up

Immortalized Panc-1 tumor cell line was used for this tumor induction and 1×10^6 cells were prepared in 500 microliters or PBS and injected subcutaneously (SC) on the back over the lateral aspect of the thigh with a 22F needle after aspirating to ensure extravascular injection. For our first injection, all animals were injected on the right side for consistency. Only local anesthesia was used for injection using 1% Lidocaine intradermal at a site at least 5 mm away from the inoculation site. The site itself was not marked. Further refining of technique led us to not "massage" the site or apply pressure so as to not have it dissipate over a wide area and have several tumors. There were no intradermal injections, so that no blebs should be visible after injection. We also made sure that the skin was mobile over the needle tract before injection so as to not inject it too deep.

The size of subcutaneous tumors was measured twice weekly and recorded. Such intensive monitoring of the tumor growth was mandated in our study since we were also trying to elicit the growth curve of the tumors. No treatment control tumors will be allowed to continue to grow when they reached >1.6 cm the animal would be euthanized if the tumor reached that size or if the animal meets the study Health Assessment of Mice criteria.[16] Animals with no tumors by 8 weeks were assessed and if healthy were re-injected on the opposite side. We had one animal, which had delayed tumor growth at the first injection site 3 months out and therefore had bilateral tumors and was excluded from the analysis.

Treatment

On the day of the procedure, the animals received 0.1 mg/kg buprenorphine SC and 0.2 mg/kg meloxicam SC prior to the end of the procedure for analgesia. The animals were weighed before the procedure and were then placed in an induction box and preoxygentated for 1 minute. The flow meter was set to between 500 and 1,000 ml/minute. The animal was kept in the induction chamber with top sealed it was ensured there was no leak. Anesthesia was then induced with Isoflurane at 3–5% via inhalation. We found it more helpful to induce them with for up to a minute after voluntary movement had ceased and until they switched to rhythmic and slow breaths. This gave us a deeper plane of anesthesia, which lasted longer and allowed us time to set up for orotracheal intubation, which lasts for about 2 minutes.

The animals were then suspended and their mouths opened by fixing their upper incisors to an intubation stand. Intubation was done with the help of BioLITE fiberoptic intubation system. The lit end of the fiberoptic cable with coupling device was connected to a 22F angiocath sheath or a mice tracheal tube. With a nontraumatic forceps, the tongue of the mouse was pulled to one side to expose the cords. The lighted tip was guided past the glottis, and the angiocath threaded into the trachea. Correct position was confirmed and the mouse was then transferred onto a warming pad, and connected to the monitoring system and ventilator Mousevent G500. The monitoring system used was MouseSTAT to monitor heart rate and pulse oximetry using tail sensor. The orotracheal tube was secured to the animal's snout with a 0 silk tie. Mechanical ventilation was maintained with 1–3% Isoflurane.

Muscle relaxation was induced with Pancuronium 0.3 mg/kg using intraperitoneal injection in the early part of the study. We later switched to using Succinylcholine at 0.05 mg/kg intraperitoneal injection. This change improved recovery, since the procedure itself did not take longer than 15–20 minutes and succinylcholine could be redosed if it went longer. Pancuronium, on the other hand, lasted close to an hour and recovery was often long with some mice going into apneic spells after recovery and dying.

After the procedure, the Isoflurane was turned off and the mouse was allowed to recover from anesthesia. T-piece with intermittent O2 was used to allow emergence from gas. We made sure the mouse was able to stand upright with the tube in place. Once motor strength was confirmed the mouse was allowed to self-extubate. It was kept under close observation for another hour before returning back to the cage and then reassessed the next morning.

The Nanoknife data entry system was used to enter animal identifiers such as room number and weight. The tumor was measured again under anesthesia in the prone position (in which the ablation would take place). We did not correct for skin-fold thickness and this remained uniform in our study. Length and breadth were measured in the largest dimensions. Depth was measured by lifting the tumor off the subcutaneous tissue whenever possible in order to get an accurate depth. These dimensions were then entered into the Nanoknife input, which would give a grid map of the ablation areas. Most human IRE probes had a greater than 1 mm diameter and although they had a protective sheath we felt the thickness of the probe to be too large for this model. Specially designed short tip electrodes (Angiodynamics, Latham, NY) were therefore used for the animal versions. Probe selection on the generator was set at two-probe array. Pulse timing was set at 90 pulses per minute (ppm) since accurate EKG synchronization was not possible in rapid mouse heart rates. Probe placement was set at 4 mm apart on the Grid.

Since a typical 2 probe array gives an oval area of ablation, tumors greater than 8 mm in largest dimension often needed >1 ablation cycles. The reason they needed >1 ablation was in order to cover the entire tumor, which in some animals was >1 cm and thus a 4 mm spacing would not cover that longest axis of the tumor. The voltage was set at 1,800–2,000 V, pulse length at 100 microseconds and number of pulses at 90. Ablation was begun with the probe in parallel to the axis of the longest dimension. After the first cycle, the leads were pulled back to ablate the remaining tumor.

Successful ablation was defined by complete delivery, which is further defined as at least 90 pulses delivered in each location, with complete coverage of the tumor in all three axes (length, width, and depth). We monitored the return resistance on the graphs after each ablation. A gradual increase in ablation resistance indicated successful ablation as established in our previous experience. Macroscopically blanching was noted over the ablated areas. Certain tumors ($N = 9$) were purposely incompletely ablated—defined as incomplete coverage of the tumor by the probes in order to assess the effects of incomplete ablation on the tumor biomarker expression. They were selected at random amongst the animals from all three injection times: RM1-1, -2, and -3.

After procedure, the animals and tumors were monitored closely for the duration of their designated observation period, up to 2 months. Special attention was paid to tumor size regression, skin ulceration, and appearance of satellite lesions or general decline in health suggestive of remote disease.

Analysis

Animal subjects were recovered and survived for 2, 7, 14, 21, 30, and 60 days prior to sacrifice and permanent fixation of tissues. Micrograph sections were prepared and stained with hematoxylin and eosin. The tumors were collected immediately after sacrifice and divided into three parts: one for hematoxylin and eosin stain, one for RT-PCR analysis and flow cytometry, and one banked. Histologic evaluation assessed for viability was also done. Recurrences were noted, voltage graphs analyzed and the tumor sent for evaluation as with the rest. Animals that worsened in BCS condition or needed to be sacrificed before reaching target timeline were also processed immediately after recovery.

In postablative animals, when two subsequent measurements indicated the increasing size of a tumor recurrence, we sacrificed these animals and analyzed the tumors for known markers of recurrence and compared them with preablation and postsuccessful ablation tumors

Tissue histology

Following harvest, tissues were serially sectioned at 5 mm intervals, fixed in 10% neutral buffered formalin and embedded in paraffin blocks. Sections were cut and stained with hematoxylin and eosin for microscopic analysis. In order to assess for areas of apoptosis, Terminal Transferase dUTP Nick End Labeling (TUNEL) Assays were performed on select sections using a In Situ Apoptosis Detection Kit (ApopTag; Intergen Company, Purchase, NY) according to the manufacturer's protocol. The TUNEL-positive cells were counted against negative cells under a light microscope at a magnification of 40×, and six visual fields were chosen on the ablated areas, areas adjacent to the ablation, and random normal pancreatic parenchyma. An apoptotic index (the number of epithelial nuclei labeled by the TUNEL method/the number of total nuclei × 100) was calculated. For EpCAM evaluation the tissues were washed with both PBS and exposed to mouse monoclonal EpCAM–FITC conjugated antibody at a 1:100 concentration for 2 hours. Thirdly, the cells were washed again with the same reagents and exposed to 1:100 concentration of mouse monoclonal Anti-CD90 antibody to identify potential tumor stem cells for 1 hour. Images were captured with a microscope (Olympus IX51-DP72 image-system, Pittsburgh, PA). All slides were blinded and review by two pathologist for tissue staining intensity.

CONFLICT OF INTEREST

[Q7]

REFERENCES

1. Bower, M, Sherwood, L, Li, Y and Martin, R (2011). Irreversible electroporation of the pancreas: definitive local therapy without systemic effects. *J Surg Oncol* **104**: 22–28.
2. Cannon, R, Ellis, S, Hayes, D, Narayanan, G and Martin, RC 2nd (2013). Safety and early efficacy of irreversible electroporation for hepatic tumors in proximity to vital structures. *J Surg Oncol* **107**: 544–549.
3. Dunki-Jacobs, EM, Philips, P and Martin, RC 2nd (2014). Evaluation of resistance as a measure of successful tumor ablation during irreversible electroporation of the pancreas. *J Am Coll Surg* **218**: 179–187.
4. Martin, RC 2nd, McFarland, K, Ellis, S and Velanovich, V (2012). Irreversible electroporation therapy in the management of locally advanced pancreatic adenocarcinoma. *J Am Coll Surg* **215**: 361–369.
5. Martin, RC 2nd, McFarland, K, Ellis, S and Velanovich, V (2013). Irreversible electroporation in locally advanced pancreatic cancer: potential improved overall survival. *Ann Surg Oncol* **20 (suppl. 3)**: S443–S449.
6. Philips, P, Hays, D and Martin, RC (2013). Irreversible electroporation ablation (IRE) of unresectable soft tissue tumors: learning curve evaluation in the first 150 patients treated. *PLoS ONE* **8**: e76260.
7. Keane, MG, Bramis, K, Pereira, SP and Fusai, GK (2014). Systematic review of novel ablative methods in locally advanced pancreatic cancer. *World J Gastroenterol* **20**: 2267–2278.
8. Narayanan, G, Hosein, PJ, Arora, G, Barbery, KJ, Froud, T, Livingstone, AS *et al*. (2012). Percutaneous irreversible electroporation for downstaging and control of unresectable pancreatic adenocarcinoma. *J Vasc Interv Radiol* **23**: 1613–1621.
9. Charpentier, KP, Wolf, F, Noble, L, Winn, B, Resnick, M and Dupuy, DE (2011). Irreversible electroporation of the liver and liver hilum in swine. *HPB (Oxford)* **13**: 168–173.
10. Charpentier, KP, Wolf, F, Noble, L, Winn, B, Resnick, M and Dupuy, DE (2010). Irreversible electroporation of the pancreas in swine: a pilot study. *HPB (Oxford)* **12**: 348–351.
11. Philips, P, Li, Y and Martin, RC 2nd (2014). Low-energy DC current ablation in a mouse tumor model. *Methods Mol Biol* **1121**: 257–265.
12. Martin, RC (2013). Irreversible electroporation of locally advanced pancreatic head adenocarcinoma. *J Gastrointest Surg* **17**: 1850–1856.
13. Lieber, M, Mazzetta, J, Nelson-Rees, W, Kaplan, M and Todaro, G (1975). Establishment of a continuous tumor-cell line (panc-1) from a human carcinoma of the exocrine pancreas. *Int J Cancer* **15**: 741–747.
14. Deer, EL, González-Hernández, J, Coursen, JD, Shea, JE, Ngatia, J, Scaife, CL *et al*. (2010). Phenotype and genotype of pancreatic cancer cell lines. *Pancreas* **39**: 425–435.
15. Philips, P, Li, Y and Martin, RC 2nd (2014). Low-energy DC current ablation in a mouse tumor model. In: Li, S, Cutrera, J, Heller, R and Teissie, J (eds.). *Electroporation Protocols*. Springer: New York. pp. 257–265.
16. Hickman, DL and Swan, M (2010). Use of a body condition score technique to assess health status in a rat model of polycystic kidney disease. *J Am Assoc Lab Anim Sci* **49**: 155–159.